Original

The Impact of Spectral Nudging on Cloud Simulation with a Regional Atmospheric Model

INSA MEINKE,* BEATE GEYER, FRAUKE FESER, AND HANS VON STORCH

Institute for Coastal Research, GKSS Research Center, Max-Planck-Strasse, Geesthacht, Germany

ABSTRACT

The impact of spectral nudging on cloud simulation with a regional atmospheric model was examined. Simulated cloudiness of the Regional Model (REMO) and the Spectrally Nudged REMO (SN-REMO) were intercompared and evaluated with satellite-derived cloudiness from the International Satellite Cloud Climatology Project (ISCCP). In general, the additional spectral nudging does not affect the mean cloud simulation. However, for particular weather regimes the introduction of spectral nudging causes notable differences in cloud simulation. Two weather conditions for these large differences in cloud simulation were derived: 1) change of the general circulation patterns, or 2) strong anticyclonic circulation within the model domain. Case studies of these weather situations indicated a better agreement of simulated and satellite-derived cloudiness when spectral nudging has been applied to the regional model.

1. Introduction

Atmospheric limited-area models need information on the governing large-scale condition. There are two different approaches to provide this information.

First, this was understood as a lateral boundary value problem. After the seminal paper of Davies (1976) on an appropriate provision of the lateral boundary information for limited-area atmospheric modeling, his "sponge zone" technique was considered the solution for regional atmospheric modeling. Now, this approach is widely used in both regional weather forecasts and regional climate applications. Although the concept is theoretically known to be ill posed, it has empirically been found to generate realistic and useful simulations.

More recently, an alternative has been suggested based on the notion that the regional climate modeling would be a downscaling problem. In this view, the large-scale state of the atmosphere is mostly known, either from analyses or from GCM simulations. The smaller scales would result from the dynamic interplay of large-scale dynamic states and physiographic detail. Technically, the spectral nudging approach (Waldron et al. 1996; von Storch et al. 2000; Weisse et al. 2000; Miguez-Macho et al. 2004) amounts to adding a term, which is proportional to the difference of the modeled and the prescribed state. This term is formulated in the spectral domain so that smaller scales are not directly affected (von Storch et al. 2000). In most cases so far, the constraint has been added into the equation of motion so that the momentum balance is no longer exactly closed, but momentum may be added, or subtracted, from one time step to the other violating the conservation of momentum. A similar problem exists with Davies' conventional method in the sponge zone. There are speculations that the correction in the sponge zone is much stronger than the continuous correction of the largest scales, but this needs to be quantified. The objective is to examine if the energy budget and the water cycle are adversely affected by the spectral nudging manipulation. More specifically, in this paper we analyze the impact of spectral nudging on the simulation of cloudiness as it is a key component of the water and energy cycle. To do so, we compare cloud statistics simulated with the regional atmospheric model REMO

* Current affiliation: Scripps Institution of Oceanography, University of California, San Diego, La Jolla, California.

Corresponding author address: Insa Meinke, Scripps Institution of Oceanography, University of California, San Diego, 9500 Gilman Drive, La Jolla, CA 92093.
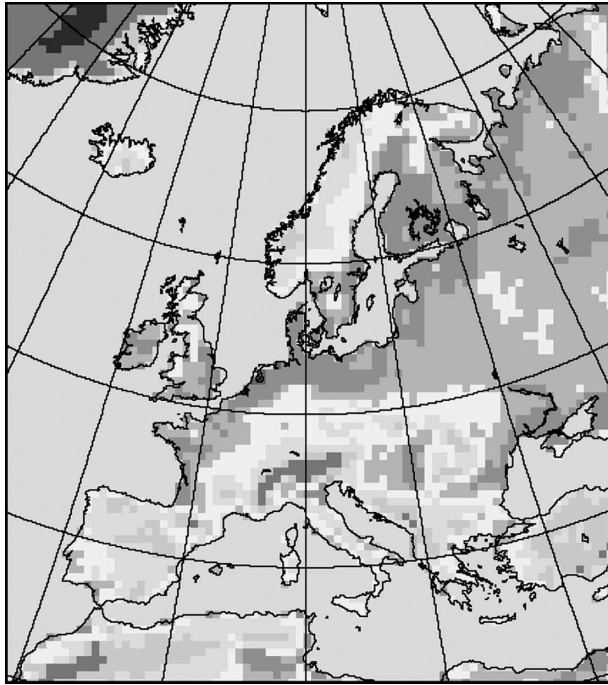E-mail: imeinke@ucsd.edu

FIG. 1. Model domain.

(Jacob and Podzun 1997) with satellite-derived cloudiness of the International Satellite Cloud Climatology Project (ISCCP) during the Pilot Study for Intensive Data Collection and Analyses of Precipitation (PIDCAP) of the Baltic Sea Experiment (BALTEX). REMO was run twice for the 3-month PIDCAP period. The two runs differ only by the presence ("SN-REMO") or absence ("REMO") of the spectral nudging technique. Otherwise, all parameterizations, dynamical formulations, and the forcing are the same for both model runs. In section 2 an experiment description as well as details of the data used is given. The main result of the model–model and model–data comparison is that spectral nudging hardly changes the mean simulated cloudiness (section 3). However, the SN-REMO simulations of particular weather situations compare better with satellite data than the simulations without spectral nudging (section 4), which is directly related to a better simulation of the large-scale hydrodynamical state of the regional atmosphere.

2. Basis of the comparison

a. Model domain and simulation period

The model domain contains Europe, the northeastern part of the North Atlantic, the North Sea, the Baltic Sea, and the Mediterranean (Fig. 1). Located at the midlatitudes the domain is impacted by frontal cyclones as well as by subtropical high pressure systems.

The model runs are carried out for August to October 1995. This period coincides with PIDCAP of BALTEX. During PIDCAP, both stratiform and convective clouds have been observed. They were connected with various weather regimes. A detailed study of the weather regimes for the whole PIDCAP period has been conducted by Isemer (1996).

b. Model configuration

Two regional model simulations were calculated for the time period from August to October 1995. The only difference between the two model runs is the application of the spectral nudging technique (von Storch et al. 2000). Thereby, the forcing is achieved by adding nudging terms in the spectral domain with maximum strength for small wavenumbers and high model levels, which are less influenced by regional structures. This method forces the regional model solution to be close to the global forcing data at large scales (>750 km), for which the highest quality in the forcing can be expected, while regional features are unconstrained. The spectral nudging forcing is introduced for the wind components above 850 hPa, increasing with height. In the following we will call the regional model simulation using the "sponge zone" technique without spectral nudging the REMO run (e.g., Jacob and Podzun 1997) and the one including spectral nudging the SN-REMO run (e.g., Meinke et al. 2004).

REMO and SN-REMO are numerical three-dimensional, hydrostatical models developed from the Europa-Modell (EM) of the Deutscher Wetterdienst (DWD, the German Weather Service; Deutscher Wetterdienst 1995; Majewski 1991) and the global model ECHAM. Parameterizations were added by Jacob and Podzun (1997). Prognostic variables of the model are surface pressure, specific humidity, liquid water, and horizontal wind components. A description on the cloud scheme and the radiation parameterization can be found in Meinke et al. (2004). The spherical coordinate system is rotated with the model equator in the center of the model domain. Thus, the horizontal grid boxes in the model area are nearly equally spaced. For the two model runs a horizontal resolution of $0.5°$ ($\sim$50 km) is used. The model domain consists of 81×91 grid boxes. The atmosphere is discretized in 20 vertical model layers in a hybrid coordinate system. The model runs were carried out in climate mode: The 6-hourly state variables, as given by the National Centers for Environmental Prediction (NCEP) global analyses (Kalnay et al. 1996), were linearly interpolated in time.
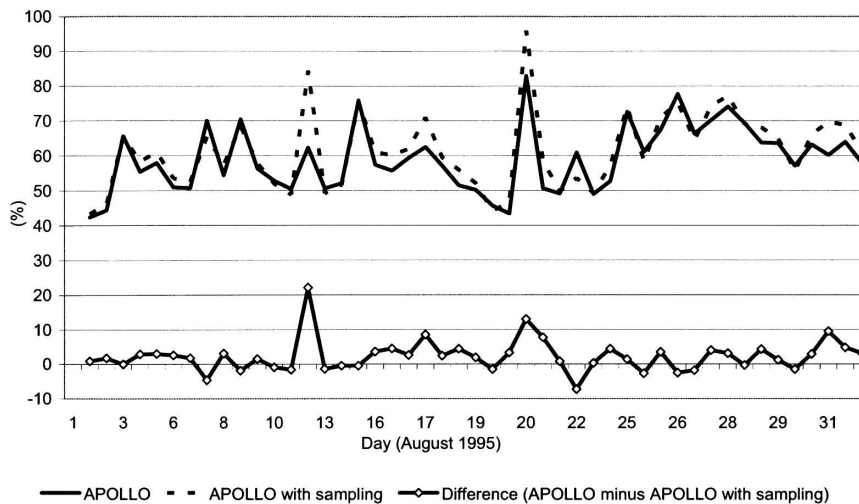
FIG. 2. Advanced Very High Resolution Radiometer (AVHRR) processing scheme over cloud, land, and ocean (APOLLO)-derived cloud fraction with and without sampling.

Every 5-min time step, they were fed into the regional model via the lateral boundaries and within the lateral sponge zone of eight grid boxes (Feser et al. 2001). In the interior of the model domain the prognostic equations are solved.

c. ISCCP data

For evaluation purposes observed data are needed. Best area coverage for cloudiness is provided by satellite data. ISCCP provides a cloud detection algorithm for surface scanning radiometers. It can be applied to polar orbiting as well as to geostationary satellites (e.g., Rossow et al. 1996). For this study the ISCCP-DX data are used. ISCCP-DX data have the highest resolution of all ISCCP products: Depending on the field of view of the infrared radiometer on various satellites the spatial resolution varies between 4 and 7 km. The following satellites were available during August to October 1995: National Oceanic and Atmospheric Administration (NOAA) satellites *NOAA-12*, *NOAA-14*, and *Meteorological Satellite-5* (*Meteosat-5*). The data of all overpasses are accumulated in 3-hourly time slots. To reduce the data volume one pixel with a resolution of the standardized field of view of the infrared radiometers is extracted once every 25 to 30 km. Figure 2 shows the difference between the full and sampled datasets. The mean difference is 2.64%. This difference, however, is not statistically significant. On the basis of the reduced dataset cloud parameters are derived. The cloud detection of ISCCP consists of two steps. First, dynamical background values for cloud-free situations are derived. On the basis of these background values threshold tests for cloud detection may be carried out in

the infrared and visible spectra. Calculating the cloud-top pressure, the cloud-top temperature is simulated in a radiation transport model (Rossow 1989). Using temperature profiles from the Television Infrared Observation Satellite (TIROS) Operational Vertical Sounder (TOVS) the corresponding cloud-top pressure is determined.

3. Comparison of time mean conditions

a. Spatial distribution of cloud amounts and cloud fraction

The spatial distributions of the time mean cloud amount (cloudy grid boxes related to all grid boxes of the domain) and cloud fraction (percentage of cloudiness in a grid box) simulated by SN-REMO and by REMO are very similar (Fig. 3). The mean space–time difference between SN-REMO and REMO is 1.1% for both cloud amount and cloud fraction. Over water surfaces the differences vary between ±4%, whereas over land surfaces the differences vary between −10% and +18%.

These data are compared to find out which model run is closer to the satellite-derived cloudiness from ISCCP. This comparison is limited to times and locations when ISCCP-DX data are available. As expected, the differences between the two model runs and ISCCP exhibit mostly the same features (Fig. 3). For cloud amount, the spatial average of time mean difference between SN-REMO and ISCCP is 1.5%, with a standard deviation of 8.3%. For REMO and ISCCP, the spatial mean difference is 0.4%; the standard deviation is 8.4%. In those
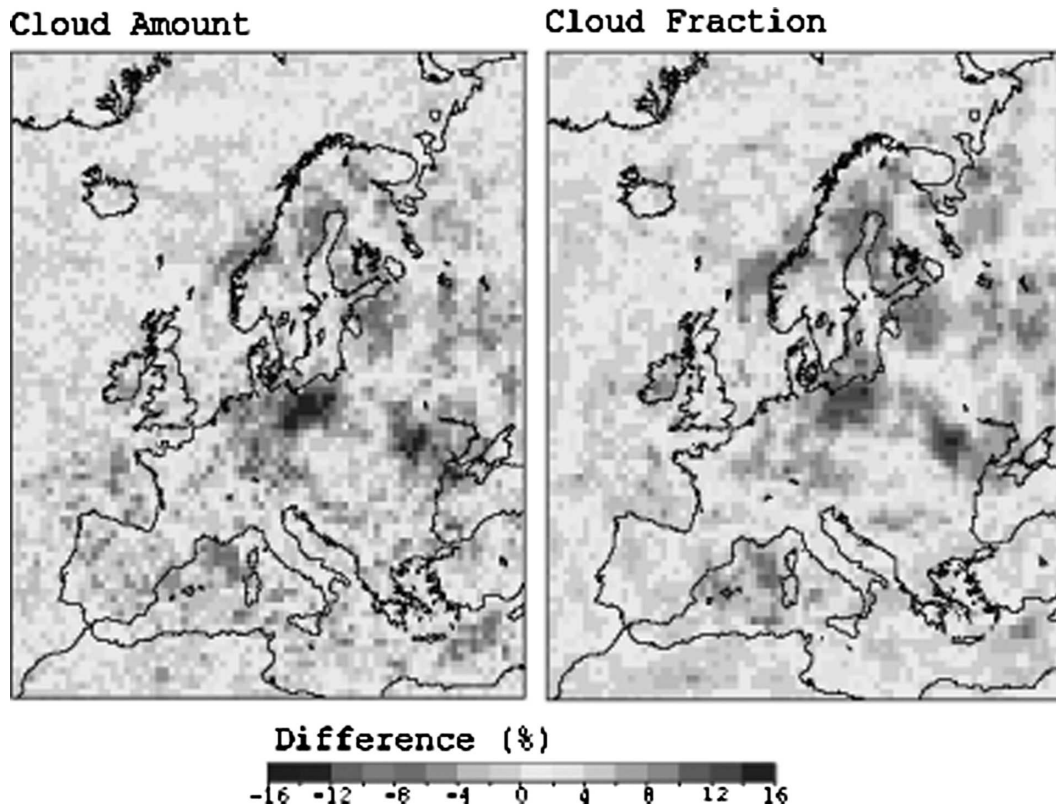
FIG. 3. Mean difference SN-REMO minus REMO in (left) cloud amount and (right) cloud fraction.

land surfaces areas, where the time mean differences between the two model runs are large (Fig. 3), the differences between SN-REMO and ISCCP are systematically smaller than the difference between REMO and ISCCP (Fig. 4).

In an earlier study (Meinke et al. 2004) a deficiency was localized in SN-REMO, namely, that too many clouds were formed. As shown above, the differences between simulated and satellite-derived cloudiness differ only slightly between the two model runs. Thus, the overgeneration of clouds is not related to the spectral nudging technique applied.

b. Mean vertical distribution at emissivity levels

Several studies have emphasized the impact of the vertical cloud distribution on the radiation budget (e.g., Chevallier and Morcrette 2000). The comparison of the vertical distribution of simulated and satellite-derived cloud amount is methodically difficult since the cloud-top pressure derived from radiances of surface scanning radiometers are representing the emissivity height of a vertical cloud column rather than the exact physical cloud-top height as simulated in a model (Meinke et al.

2004). Hence, to compare with ISCCP data, the emissivity heights of the simulated cloud columns have to be calculated. This emissivity height is that pressure level, whose corresponding temperature is the same as the brightness temperature of the vertical cloud column (Meinke et al. 2004). The brightness temperature of the simulated vertical cloud column is calculated after the delta-Eddington approximation (Wiscombe 1977; Slingo and Schrecker 1982; Slingo 1989). As the calculation of cloud properties in SN-REMO and REMO is based on the center of each model layer with varying thicknesses of between 5 and 100 hPa, 20 emissivity levels can be distinguished. Figure 5 shows the space–time mean differences between simulated and satellite-derived cloud amounts on emissivity levels on the left. On the right the space–time mean differences between SN-REMO and REMO simulated cloud amount are indicated.

As already found in the earlier study (Meinke et al. 2004), SN-REMO overestimates cloud amounts at low-level emissivity heights (1000–475 hPa) whereas at high-level emissivity heights (<475 hPa) cloud amounts are underestimated (Meinke et al. 2004). The same pattern holds for the differences between REMO and
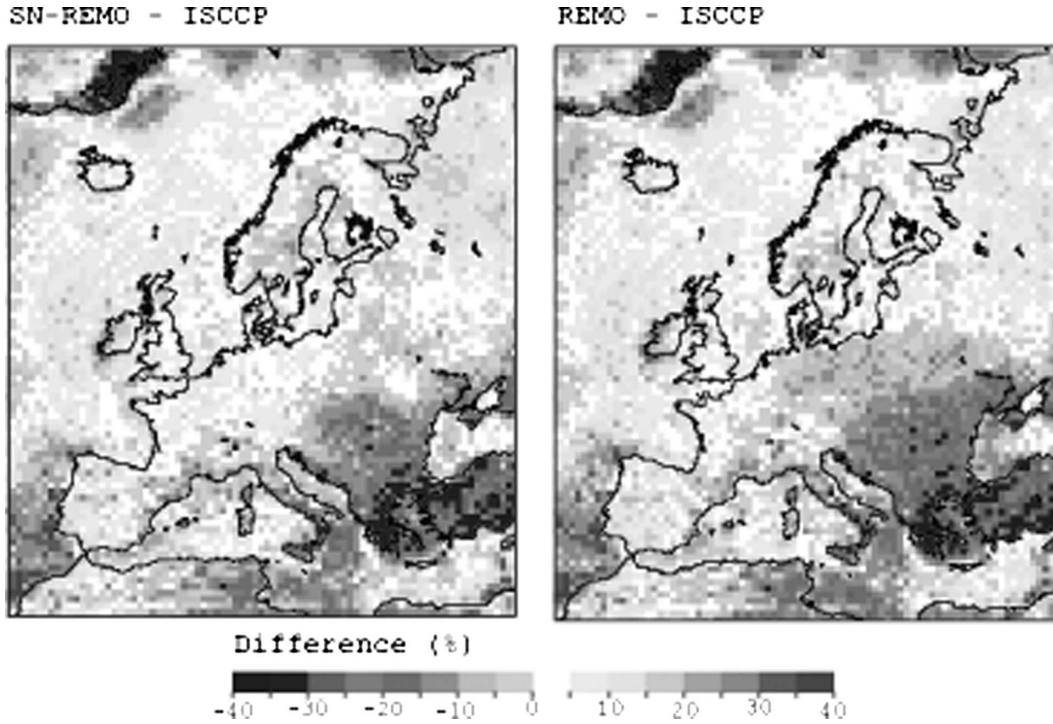
FIG. 4. Mean difference between simulated and satellite-derived cloud amount. (left) SN-REMO minus ISCCP and (right) REMO minus ISCCP.

ISCCP (Fig. 5). The difference between SN-REMO and REMO is quite small (Fig. 5, right) and not statistically significant at any emissivity level.

We conclude that the introduction of the spectral nudging into REMO has practically no influence on the performance of the model in terms of time-mean cloud amounts, cloud fraction, and the time mean vertical distribution of clouds.
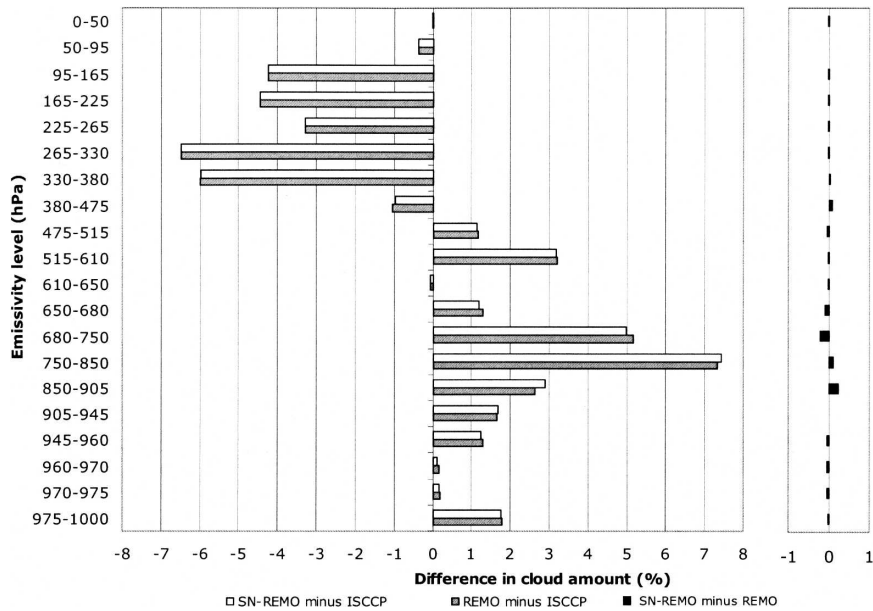

FIG. 5. Temporal area mean of the difference in cloud amount vs emissivity levels averaged over the integration domain (without sponge zone).

4. Temporal variation of simulated cloud properties

a. Spatial means

Figure 6 shows the temporal variation of the spatially averaged root-mean-square (rms) differences between SN-REMO and REMO in terms of cloud amount and cloud fraction. The maximum differences are 12.4%, with a mean value of 3.2% in terms for cloud amount, and 9.3% with a mean value of 2.8% for cloud fraction.

For identifying plausible reasons for the sometimes large differences, we determined the periods when the differences were largest. In particular, we determined a threshold of the cloud amount rms differences, so that 10% of all differences were above that threshold. This threshold was found to be of 7.35%. For these 36 largest differences the root-mean-square differences of SN-REMO versus ISCCP and REMO versus ISCCP are shown in Fig. 7. In 83.33% of these cases the differences between SN-REMO and ISCCP are smaller than the differences between REMO and ISCCP. The mean difference of SN-REMO minus ISCCP is 9.65% and 16.26% for the difference between REMO and ISCCP. For all cases the difference between SN-REMO and ISCCP is 10.72%, and between REMO and ISCCO the difference is 12.16%. This shows that spectral nudging improves the simulation.

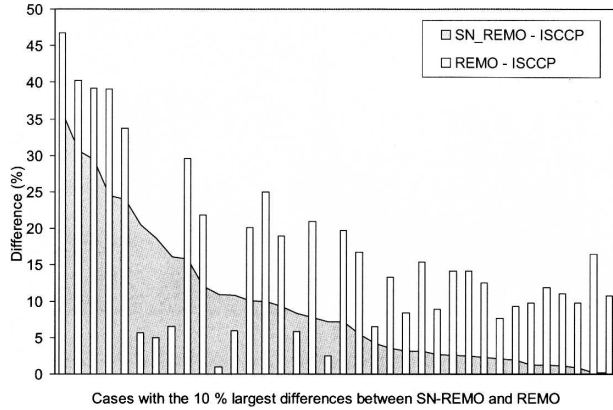The 36 largest differences between SN-REMO and

FIG. 7. Rms differences SN-REMO vs ISCCP and REMO vs ISCCP of the 10% largest differences between SN-REM0 and REMO (see Fig. 6).

REMO are concentrated on 14 days. These days belong to 8 different weather regimes (see Table 1 and Fig. 6), which are characterized by one of the following two conditions:

1) change of the general circulation patterns (cases 2, 3, 5, and 8) or
2) strong anticyclonic circulation within the model area (cases 1, 4, 6, and 7).

Both conditions represent situations where a major impact of spectral nudging on the regional simulation is
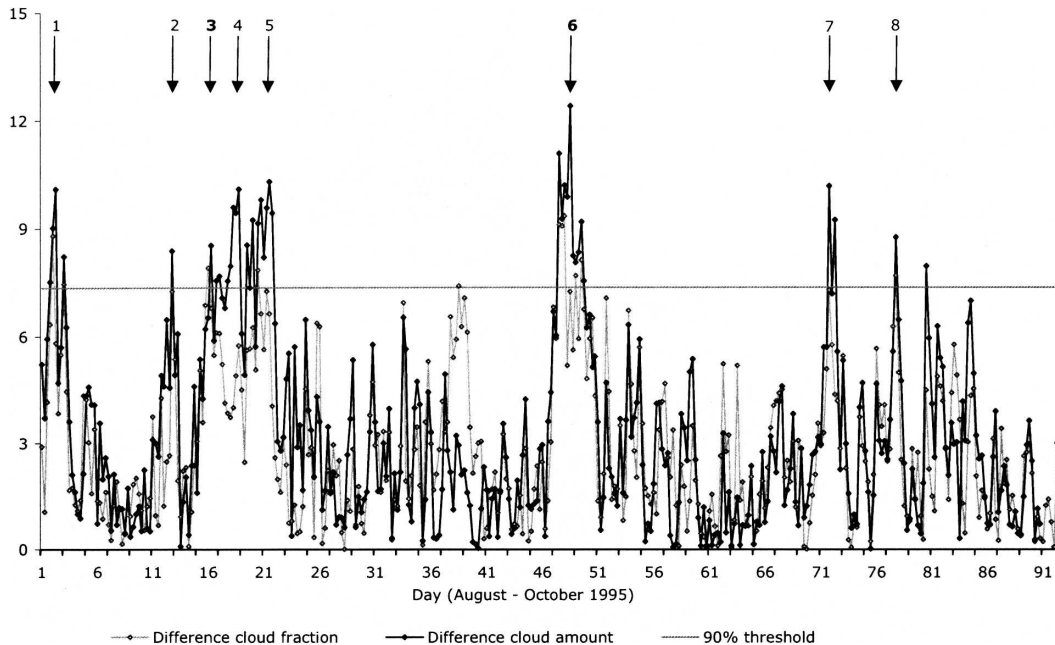

FIG. 6. Rms differences in cloud fraction (light gray line) and cloud amount (solid black line) between SN-REMO and REMO. The horizontal gray line represents a threshold, so that 10% of all cases are above and 90% are below. The vertical arrows mark the eight cases listed in Table 1.

TABLE 1. Weather situations enlarging the difference between SN-REMO and REMO.

No.	Date in 1995	Weather regime
1	2–3 Aug	An extended anticyclone located over central Scandinavia moved slowly eastward.
2	13 Aug	Change from anticyclonic circulation to cyclonic activity: A small surface cyclone developed over the area between Faroe Islands and Norway. This cyclone was connected with a midtropospheric trough.
3	16 Aug	Change to anticyclonic circulation. The cyclone was moving eastward while an anticyclone over Great Britain, France, and Germany extended eastward into the model area.
4	18–21 Aug	Anticyclonic circulation patterns were predominating this period. A weak cold front of an arctic cyclone crossed the model area from north to south during this time span.
5	22 Aug	Change of the general weather situation in the model area toward stronger cyclonic activity and more variable weather patterns.
6	16–18 Sep	Extended anticyclone over Scandinavia moved slowly southeastward. The related anticyclonic circulation patterns dominated over Scandinavia during this period. The influence of these anticyclonic circulation patterns weakened after 18 Sep.
7	11 Oct	An extended midtropospheric anticyclone located over mid- and southern Europe was dominating the circulation patterns.
8	17 Oct	Change of circulation to more cyclonic activity. The influence of the anticyclone weakened.

expected: During an anticyclonic regime, the through-flow of weather systems is blocked, and the state in the interior of the model domain becomes detached from the lateral forcing in the REMO run. Also, when a fast change of the circulation pattern takes place, REMO has more freedom to develop differently from the real situation. The spectral nudging, however, enforces the regional model solution to remain close to the large-scale global forcing. Thus, additional information on changes in the general weather situation is provided to the regional model; diminishing influence of the lateral boundary conditions is of little importance, as the large scale is imposed on the interior as well. Therefore, differences between SN-REMO and REMO are most probable in these weather situations.

b. Case studies

For each of these two weather situations associated with large differences between SN-REMO and REMO one case was chosen to compare with ISCCP data, that is, 16 August 1995 (case 3, Table 1) and 17 September 1995 (case 6, Table 1), respectively. The other six cases show similar results, namely, that the introduction of spectral nudging improves the capability of the model to reproduce the satellite-derived cloud distributions.

The condition of 16 August 1995 is an example of a change in the general weather regime (case 3, Table 1). Figure 8 (top) shows the sea level pressure maps of SN-REMO (left), the DWD analyses (middle), and REMO (right). The SN-REMO map corresponds closely to the independent routine analysis by the DWD, but the REMO simulation deviates significantly in some parts of the domain. The most obvious difference is the larger extension and higher pressure of the anticyclone over Great Britain in the REMO run. In

accordance with reality, SN-REMO calculates a less extended anticyclone, so that low pressure systems in the southeast are situated more westward within the model domain than in the REMO run.

Comparing simulated and satellite-derived clouds by and large, the SN-REMO cloud fraction compares favorably with the ISCCP cloud fraction, while REMO fails to simulate significant parts of the pattern (Fig. 8, bottom): In the western part of the model area, both models simulate more cloudiness than was derived by ISCCP, especially in the northern part of the model domain. This is in accordance with the sea level pressure, which is nearly the same for SN-REMO and REMO in the northern part of the model area. In the eastern part, however, the SN-REMO cloud fraction pattern matches ISCCP much better than REMO. In the southeast, many clouds are detected by ISCCP, which are mostly well reproduced by SN-REMO, while the region is almost cloud free in REMO. These clouds are connected with an occlusion of a cyclone moving eastward. The different cloud simulations of SN-REMO are related to different circulation patterns described above. But also in SN-REMO significant differences to ISCCP emerge, such as some cloud-free areas in northeastern Germany and western Poland, and over south Italy and Greece. Nonetheless, spectral nudging improves especially the simulation of cloudiness associated with that low pressure system moving eastward.

The other example deals with the strong anticyclonic circulation on 17 September 1995 (case 6, Table 1; Fig. 9). The circulation patterns of this case show major differences regarding exposure and pressure of the anticyclone over Scandinavia and the Baltic Sea: The anticyclone simulated by REMO is situated more north-eastward and has a smaller extension and lower pres-
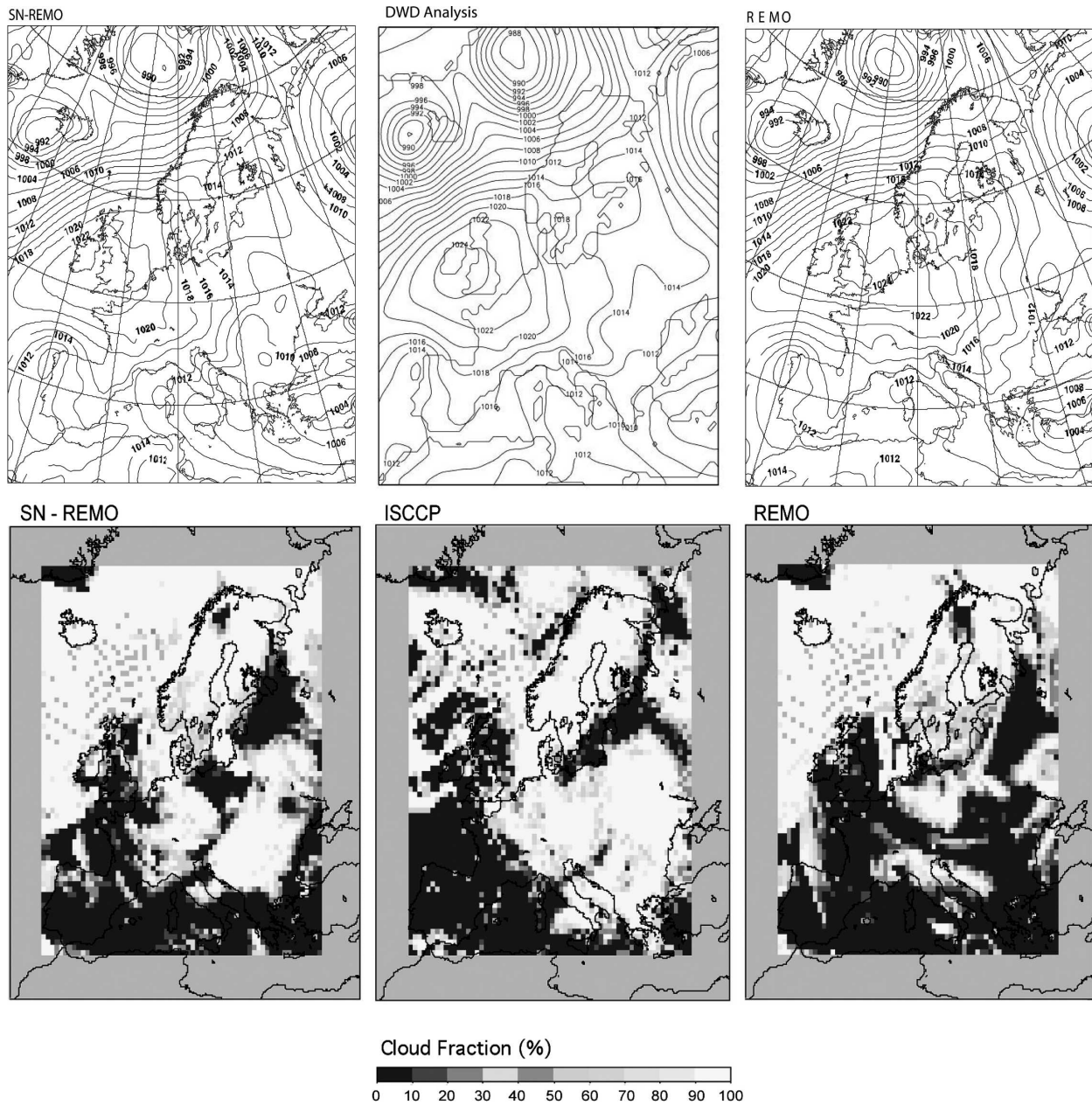
FIG. 8. The case of 0600 UTC 16 Aug 1995. (top) Sea level pressure (hPa) simulated by (left) SN-REMO and (right) REMO and (middle) the DWD analyses as reference. (bottom) Cloud fraction simulated by (left) SN-REMO, (middle) recorded by ISCCP, and (right) simulated by REMO. The sponge zone is given by the gray margin.

sure than the high pressure system calculated by SN-REMO, which matches the objective DWD analysis well (Fig. 9, middle). Consequently, the exposure of the cold front between this anticyclone and the low pressure system northeast from the Crimean peninsula differs as well.

Similar to the previous case, both model versions overpredict the presence of clouds over the Atlantic

Ocean. Also in this case, this is in accordance with similar circulation patterns of both model runs in that area. In the eastern part of the model area there is a good agreement in cloud distribution between SN-REMO and ISCCP. Corresponding to the prevailing extended anticyclone over Scandinavia and the Baltic Sea there is a large cloud-free area, which is well simulated by SN-REMO even if the simulated cloud-free area is a bit too
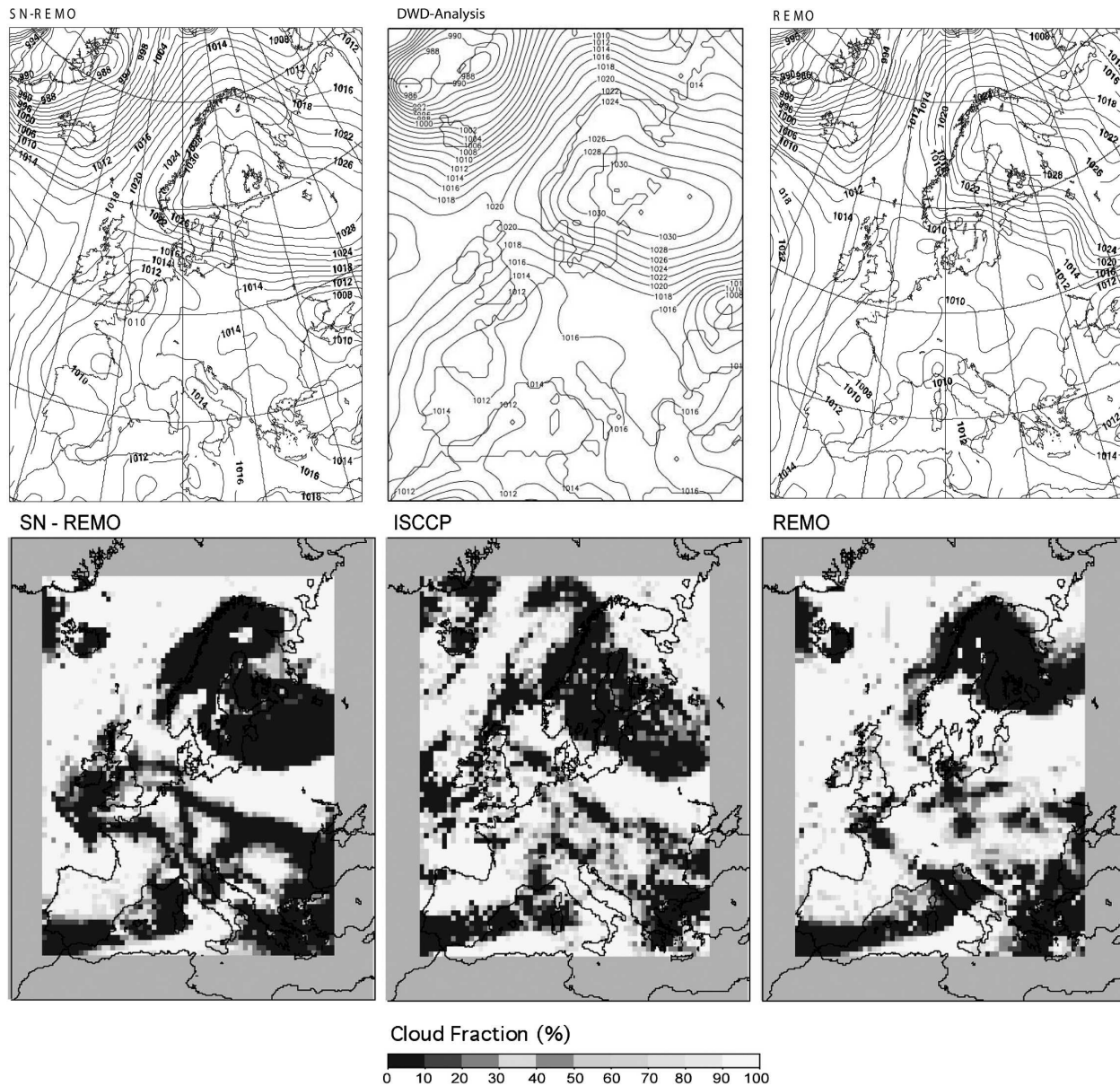
FIG. 9. The case of 17 Sep 1995. (top) Sea level pressure (hPa) simulated by (left) SN-REMO and (right) REMO and (middle) the DWD analyses as reference. (bottom) Cloud fraction simulated by (left) SN-REMO, (middle) recorded by ISCCP, and (right) simulated by REMO. The sponge zone is given by the gray margin.

large. REMO simulates just a small cloud-free area situated more northeastward than the one in ISCCP. Another ISCCP feature is the cold front over Denmark, Poland, Ukraine, and Russia with a broad cloud band; also this feature is captured by SN-REMO but not by REMO. On the rear of the cold front cloud-free areas alternate with cloudy regions. The cloud-free areas simulated by SN-REMO in that region are larger than those detected by ISCCP. However, their cloud distributions are similar. As in the first case, the differ-

ent performance of SN-REMO and REMO in simulating cloud distributions is connected with the different circulation patterns of SN-REMO and REMO as discussed above.

Also in this example the simulation is improved with spectral nudging. Improvements occur especially in the simulation of cloud-free areas connected with the anticyclone over Scandinavia and cloudiness associated with the cold front over the southeastern part of the model area.

5. Discussion

Intercomparisons between SN-REMO and REMO were conducted regarding the mean cloud distribution, the mean distribution of clouds at emissivity levels, and the temporal distribution of cloud area means. Results of these comparisons show that spectral nudging does not affect the mean simulation of cloudiness with a regional model. For cloud fraction and cloud amount the mean differences of the spatial distribution between the two model runs is 1.1%. In some areas over land surfaces the difference between the two model runs are markedly larger than on average. In these areas the difference between SN-REMO and ISCCP is smaller than between REMO and ISCCP. The mean cloud distribution at emissivity levels shows almost no difference between the two model runs. Consequently, they have nearly the same differences to the satellite-derived clouds from ISCCP. Thus, earlier noted deficiencies of this model regarding the simulation of cloudiness (Meinke et al. 2004) are not caused by the introduction of spectral nudging but are a property of the parameterizations of physical processes in the used model. Since spectral nudging is strongest at upper levels it may have been suspected that spectral nudging negatively interferes with the formation of high clouds. However, our analysis has shown that the systematic errors in REMO and SN-REMO are almost identical in all levels.

The temporal variation of rms differences between the two models is intermittently large, in particular, when one of two conditions is met: 1) change of the general circulation patterns, or 2) strong anticyclonic circulation in the model area. Case studies (one for each condition is shown) indicated that spectral nudging leads to a higher accordance with operational analyses and satellite-derived data. Both conditions meet expectations on how spectral nudging impacts regional modeling as additional information on large-scale circulation. The spectral nudging enforces the regional model solution to remain close to the large-scale global forcing. Applying the "sponge zone" technique, however, the regional model has more freedom to develop differently from the real situation in the interior model domain.

REFERENCES

Chevallier, F., and J.-J. Mocrette, 2000: Comparison of model fluxes with surface and top of the atmosphere observations. ECMWF Tech. Memo. 300, 25 pp.

Davies, H. C., 1976: A lateral boundary formulation for multilevel prediction models. *Quart. J. Roy. Meteor. Soc.,* **102,** 405–418.

Deutscher Wetterdienst, Ed., 1995: Dokumentation des EM/DM systems. Offenbach/Main, Germany, 492 pp.

Feser, F., R. Weisse, and H. von Storch, 2001: Multi decadal atmospheric modeling for Europe yields multi purpose data. *Eos, Trans. Amer. Geophys. Union,* **82,** 305–310.

Isemer, H.-J., 1996: Weather patterns and selected precipitation records in the PIDCAP period, August to November 1995. GKSS External Rep. 96/E/55, 92 pp.

Jacob, D., and R. Podzun, 1997: Sensitivity studies with the Regional Model REMO. *Meteor. Atmos. Phys.,* **63,** 119–129.

Kalnay, E., and Coauthors, 1996: The NCEP/NCAR 40-Year Reanalysis Project. *Bull. Amer. Meteor. Soc.,* **77,** 437–471.

Majewski, D., 1991: The Europa Model of the Deutscher Wetterdienst. *Proc. Seminar on Numerical Methods in Atmospheric Models,* Vol. 2, Reading, United Kingdom, ECMWF, 147–191.

Meinke, I., H. von Storch, and F. Feser, 2004: A validation of the cloud parameterization in the regional model SN-REMO. *J. Geophys. Res.,* **109,** D13205, doi:10.1029/2004JD004520.

Miguez-Macho, G., G. L. Stenchikov, and A. Robock, 2004: Spectral nudging to eliminate the effects of domain position and geometry in regional climate model simulations. *J. Geophys. Res.,* **109,** D13104, doi:10.1029/2003JD004495.

Rossow, W., 1989: Measuring cloud properties from space: A review. *J. Climate,* **2,** 201–213.

——, A. Walker, and M. Roiter, 1996: International Satellite Cloud Climatology Project (ISCCP) documentation of new cloud datasets. WMO Tech. Doc. 737, 115 pp.

Slingo, A., 1989: A GCM parameterization for the shortwave radiative properties of water clouds. *J. Atmos. Sci.,* **46,** 1419–1427.

——, and H. Schrecker, 1982: On the shortwave radiative properties of stratiform water clouds. *Quart. J. Roy. Meteor. Soc.,* **108,** 407–426.

von Storch, H., H. Langenberg, and F. Feser, 2000: A spectral nudging technique for dynamical downscaling purposes. *Mon. Wea. Rev.,* **128,** 3664–3673.

Waldron, K. M., J. Peagle, and J. D. Horel, 1996: Sensitivity of a spectrally filtered and nudged limited area model to outer model options. *Mon. Wea. Rev.,* **124,** 529–547.

Weisse, R., H. Heyen, and H. von Storch, 2000: Sensitivity of a regional atmospheric model to a sea state dependent roughness and the need of ensemble calculations. *Mon. Wea. Rev.,* **128,** 3631–3642.

Wiscombe, W., 1977: The Delta-Eddington approximation for a vertically inhomogeneous atmosphere. NCAR Tech. Note NCAR/TN-121+STR, 66 pp.